Methyl (11a*S*)-1,2,3,5,11,11a-Hexahydro-3,3-dimethyl-1-oxo-6*H*-imidazo-[3′,4′:1,2]pyridin[3,4-*b*]-indol-2-Substituted Acetates: Synthesis and Three-Dimensional Quantitative Structure−Activity Relationship Investigation as a Class of Novel Vasodilators

Jiawang Liu, Ming Zhao,* Guohui Cui, Xiaoyi Zhang, Jun Wang, and Shiqi Peng*

College of Pharmaceutical Sciences, Capital Medical University, Beijing 100069, PR China

Received March 7, 2008

To find selective inhibitor of phosphodiesterase type 5 (PDE5), the essential structure elements of clinically used drugs sildenafil, vardenafil, and tadalafil were combined and a tetracyclic parent was constructed to which in 2-positions substituted acetic acid methylesters were introduced to form 17 novel vasodilators, methyl (11a*S*)-1,2,3,5,11,11a-hexahydro-3,3-dimethyl-1-oxo-6*H*-imidazo[3′,4′:1,2]- pyridin[3,4-*b*]indol-2-substituted acetates. By molecular field analysis (MFA), an equation of three-dimensional quantitative structure−activity relationship (3D QSAR) was established, which not only revealed the dependence of the in vitro vasorelaxation activities on the structures but also pointed out the way to design new lead compounds properly. Docking these novel vasodilators into the hydrophobic pocket of phosphodiesterase type 5 (PDE5) revealed that their adaptabilities to this pocket did significantly affect on their vasorelaxation activity. Actually, the docking adaptabilities of these novel vasodilators to PDE5 were consistent with the conformational requirements of them to MFA and with the crystal conformation of two representatives.

Introduction

Regardless of the initiating process, cardiovascular disease,[1] sickle cell disease,[2] cerebral vasospasm,[3] stroke,[4] ischemic heart disease,[5] and atherosclerosis[6] manifest themselves as the most common causes of death in developed countries and represent a substantial burden to the healthcare systems around the world. For instance, cardiac infarction alone may be responsible for about 30% of all deaths of cardiovascular disease in some countries. In these diseases, properties of blood vessels are usually changed, which may be the results of vasoconstriction.

Vasoconstriction may result in disturbances of the vascular tone and blood flow and subsequently spread the supply of organs' oxygen and nutrients. Discovering vasorelaxation substances have been of importance and attracted a number of interests. A series of endogenous substances are involved in vasorelaxation, among which cyclic adenosine monophosphate (cAMP)[a] and cyclic guanosine monophosphate (cGMP) play a critical role.[7–9] Increasing the concentration of cAMP and cGMP causes the activation of protein kinase A and protein kinase G, which phosphorylate a variety of substrates regulating a myriad of physiological processes including cardiac and smooth muscle contraction.[10] Besides, phosphodiesterases (PDEs) hydrolyze cAMP and cGMP into 5′-nucleotide monophosphates and consequently regulate their cellular levels. PDE inhibition may block phosphodiester hydrolysis and result in higher levels of cyclic nucleotides. Thus PDE inhibitors may have a large variety of therapeutic utilities including vasodilators.[11,12] PDEs consist of 11 classes of human cyclic nucleotide phosphodiesterases, among which the PDE5 enzyme is selective for cGMP.[13,14] PDE5 is importantly expressed in human corpus cavernosum tissue.[15] In the literature, three PDE5 inhibitors sildenafil,[16] vardenafil,[17] and tadalafil[18] were reported to be capable of treating erectile dysfunction. Their structures are shown in Figure 1.

The high-resolution cocrystal structures of PDE5 and inhibitors reveal its active site as a pocket having a surface area of approximately 675 Å^2 and a volume of 927 Å^3.[19] This pocket has a narrow side as its hydrophobic clamp and a wider side as its binuclear metal ion center. These lead to a structural requirement for the inhibitor bound to PDE5, that is, the inhibitor should contain a planar heterocyclic ring that is not only capable of sandwiching into the hydrophobic clamp but also forming an H bond with Q817. To meet this requirement, 17 novel methyl (11a*S*)-1,2,3,5,11,11a-hexahydro-3,3-dimethyl-1-oxo-6*H*-imidazo[3′,4′:1,2]pyridin[3,4-*b*]indol-2-substituted acetates were designed here. We hope that they interact as vasorelaxation agents with the metal ions mediated through water, the protein residues involved in nucleotide recognition and the hydrophobic residues lining the cavity of the active site. Therefore, their in vitro vasodilation assay, molecular field analysis (MFA), and docking studies were performed. Besides, the crystal structures of two compounds **4f**,**h** were also reported in this study.

Results and Discussion

Synthesis of 4a−q. The synthetic route of methyl (11a*S*)-1,2,3,5,11,11a-hexahydro-3,3-dimethyl-1-oxo-6*H*-imidazo[3′,4′:1,2]pyridin[3,4-*b*]indol-2-substituted acetates (**4a−q**) is summarized in Scheme 1. At 0 °C, (*S*)-2-(*tert*-butoxycarbonyl)-2,3,4,9-tetrahydro-1*H*-pyrido-[3,4-*b*]indole-3-carboxylic acid were coupled with L-amino acid methylesters providing substituted (*S*)-*tert*-butyl 3-(2-methoxy-2-oxoethylcarbamoyl)-3,4-dihydro-1*H*-pyrido[3,4-*b*]indole-2(9*H*)-carboxylate **3a−q** in 76−99% yields. After removing the *tert*-butoxycarbonyl (Boc) group, the formed substituted (*S*)-*tert*-butyl 3-(2-methoxy-2-oxoethylcarbamoyl)-3,4-dihydro-1*H*-pyrido[3,4-*b*]indole-2(9*H*)-carboxy-

* To whom correspondence should be addressed. For S.P.: Phone, 86-10-8391-1528; Fax, 86-10-8391-1528; E-mail, sqpeng@mail.bjmu.edu.cn. For M.Z.: Phone, +86 10 8280 2482; fax, +86 10 8280 2482; E-mail,mingzhao@mail.bjmu.edu.cn.

[a] Abbreviations: 3D-QSAR, three-dimensional quantitative structure−activity relationship; PDEs, phosphodiesterases; PDE5, phosphodiesterase type 5; MFA, molecular field analysis; Boc, *tert*-butoxycarbonyl; DMSO, dimethyl sulfoxide; NE: noradrenaline; THF: tetrahydrofuran; HOBt: *N*-hydroxybenzotriazole; DCC: dicyclohexylcarbodiimide; DMF, *N*,*N*-dimethyl formamide; NMM, *N*-methyl morpholine; MCS, maximum common subgraph; G/PLS, genetic partial least-squares; TLC, thin layer chromatography; cAMP, cyclic adenosine monophosphate; cGMP, cyclic guanosine monophosphate; Ach, acetylcholine

10.1021/jm800249j CCC: $40.75
Published on Web 07/11/2008

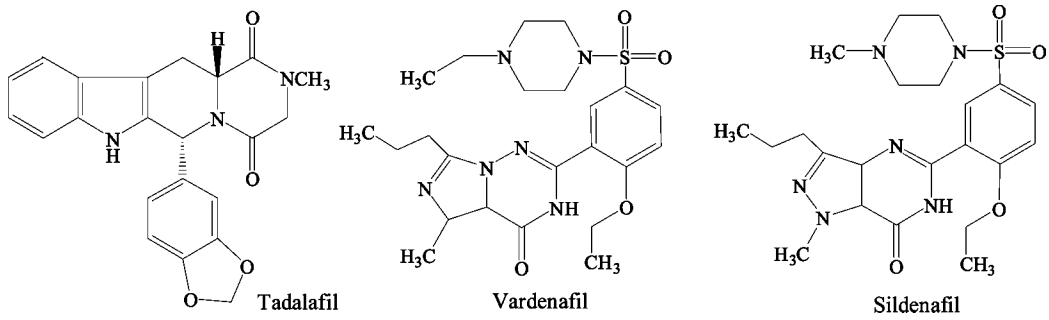

Figure 1. Structures of three PDE5 inhibitors.

Scheme 1. Synthetic Route of Methyl (11a*S*)-1,2,3,5,11,11a-hexahydro-3,3-dimethyl-1-oxo-6*H*-imidazo-[3′,4′:1,2]pyridin[3,4-*b*]indol-2-Substituted Acetates[a]

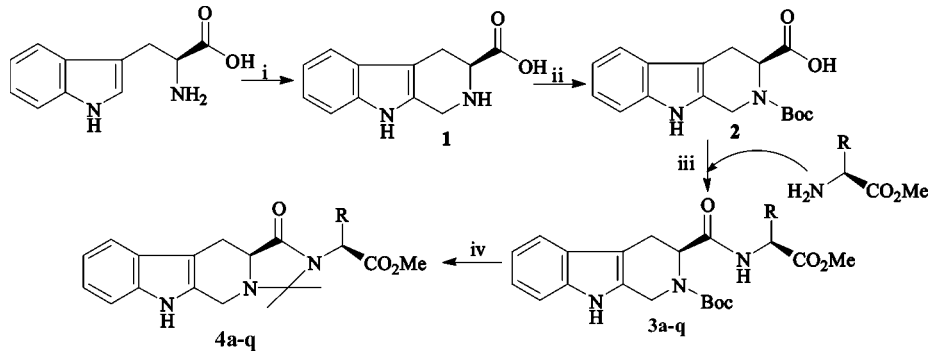

[a] (i) Formaldehyde and sulfuric acid. (ii) $(Boc)_2O$, DMF. (iii) DCC, HOBt, NMM. (iv) Hydrogen chloride in ethyl acetate (4N), methanol, acetone, triethylamine. In **3a**,**4a** R = $CH(CH_3)CH_2CH_3$; **3b**,**4b** R = $CH(CH_3)_2$; **3c**,**4c** R = $CH_2CH(CH_3)_2$; **3d**,**4d** R = CH_3; **3e**,**4e** R = H; **3f**,**4f** R = $CH_2C_6H_5$; **3g**,**4g** R = $CH_2C_6H_4$−OH-p; **3h**,**4h** R = indole-3-ylmethyl; **3i**,**4i** R = CH_2CO_2Me; **3j**,**4j** R = $CH_2CH_2CO_2Me$; **3k**,**4k** R = CH_2OH; **3l**,**4l** R = $CH(OH)CH_3$; **3m**,**4m** R = CH_2CONH_2; **3n**,**4n** R = $CH_2CH_2CONH_2$; **3o**,**4o** R = $CH_2CH_2CH_2NHC(NH)NH_2$; **3p**,**4p** R = imidazole-4-ylmethyl; **3q**,**4q** R = $CH_2CH_2SCH_3$.

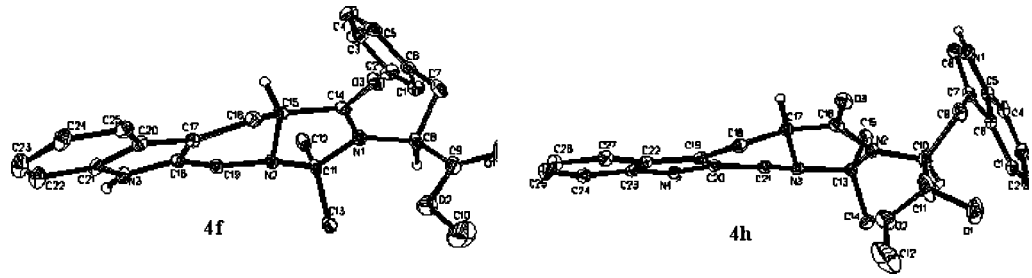

Figure 2. ORTEP representation of **4f** and **4h**, the vasodilation inactive and active compounds.

late were directly treated with acetone to give methyl (11a*S*)-1,2,3,5,11,11a-hexahydro-3,3-dimethyl-1-oxo-6*H*-imidazo[3′,4′:1,2]pyridin[3,4-*b*]indol-2-substituted acetates in 35−65% total yields. These results suggest that a two-step-procedure with a simple wash is able to provide the goal products satisfactorily.

Crystal structures of 4f,h. Two single crystals of **4f**, the vasorelaxation inactive compound with benzyl side chain, and **4h,** the vasorelaxation potent compound with indole-3-ylmethyl side chain, were prepared by evaporating their dimethyl sulfoxide (DMSO) solutions. Their crystal structures were determined by X-ray diffractometry and the intensities were collected at 291.2 K on a Rigaku Raxis2IV diffractometer with graphite monochromated Mo Kα radiation (λ = 0.71073 Å). The data collection, cell refinement, and reduction were carried out with SMART and SAINT programs. Software used for structure solution, refinement, analysis, and drawing include SHELXL97, SHELXL97 all handled by the WINGX package.

Their crystal data are given as Supporting Information. Their ORTEP representations in Figure 2 show the molecular structures and the atom numbering schemes.[20] As seen from Figure 2, the orientation of the 2-benzyl of vasorelaxation inactive **4f** is different from that of the 2-indole of vasorelaxation active **4h**, the benzyl group points the upper face of the 1,2,3,5,11,11a-hexahydro-3,3-dimethyl-1-oxo-6*H*-imidazo- [3′,4′:1,2]pyridin[3,4-*b*]indole ring, while the indole group points the under face of this ring. The distinct orientations of 2-benzyl and indole groups and various vasorelaxation activities of **4f**,**h** imply that the conformations of the 2-substituents of **4a**−**q** greatly affect their vasorelaxation activities.

Vasorelaxation Activities of 4a−q. To examine the vasorelaxation activities of **4a**−**q**, the in vitro vasodilation assays were performed and the data are listed in Table 1. These assays explored that 59 μM of noradrenaline (NE) induced hypertonic contraction of the vessel strip may be effectively counteracted by 50 μM of **4a**,**d**,**e**,**h**,**o**. It was also found that, compared to the reference compound acetylcholine (Ach), **4d**,**h** were more potential, and compared to the reference drug tadalafil, **4d** was equally active. However, these activities were from the preliminary in vitro evaluations and the in vivo assays remain to

Table 1. Effect of **3a**−**q** and **4a**−**q** on NE Induced Vasoconstriction[a]

R	compd	vasorelaxation	compd	vasorelaxation
$CH(CH_3)CH_2CH_3$	**3a**	10.9 ± 1.9	**4a**	34.0 ± 4.3[e]
$CH(CH_3)_2$	**3b**	8.9 ± 1.4	**4b**	24.2 ± 1.8
$CH_2CH(CH_3)_2$	**3c**	7.8 ± 2.7	**4c**	15.7 ± 1.6
CH_3	**3d**	18.8 ± 2.2	**4d**	91.8 ± 5.6[b,f]
H	**3e**	13.5 ± 1.7	**4e**	45.5 ± 3.2[d]
$CH_2C_6H_5$	**3f**	0	**4f**	0
$CH_2C_6H_4$-OH-p	**3g**	7.4 ± 2.6	**4g**	16.3 ± 1.5
indole-3-ylmethyl	**3h**	15.2 ± 2.1	**4h**	63.5 ± 4.4[c,f]
$CH_2CO_2CH_3$	**3i**	0	**4i**	6.3 ± 1.6
$CH_2CH_2CO_2CH_3$	**3j**	0	**4j**	9.9 ± 2.1
CH_2OH	**3k**	6.1 ± 1.8	**4k**	16.9 ± 1.2
$CH(OH)CH_3$	**3l**	0	**4l**	0
CH_2CONH_2	**3m**	0	**4m**	0
$CH_2CH_2CONH_2$	**3n**	0	**4n**	0
$(CH_2)_3NHC(NH)NH_2$	**3o**	11.3 ± 1.9	**4o**	36.7 ± 3.1[e]
imidazole-4-ylmethyl	**3p**	0	**4p**	0
$CH_2CH_2SCH_3$	**3q**	6.0 ± 2.4	**4q**	15.1 ± 2.0
	tadalafil	89.9 ± 5.2[b]	Ach[g]	42.3 ± 2.9[d]
	ethanol	0		

[a] Vasorelaxation activity is represented by the percent of NE induced hypertonic contraction of the vessel strip X ± SD%, $n = 6$; final concentration: **3a**−**q** = 5 mM, **4a-q** = 50 μM, tadalafil, Ach = 50 μM. [b] Compared to **4a**−**c**,**e**−**q** $P < 0.01$. [c] Compared to **4a**−**c**,**e**−**g**,**i**−**q** $P < 0.01$. [d] Compared to **4a**−**c**,**f**,**g**,**i**−**q** $P < 0.01$. [e] Compared to **4b**,**c**,**e**−**g**,**i**−**n**,**q** $P < 0.01$. [f] Compared to Ach $P < 0.01$. [g] Ach: acetylcholine.

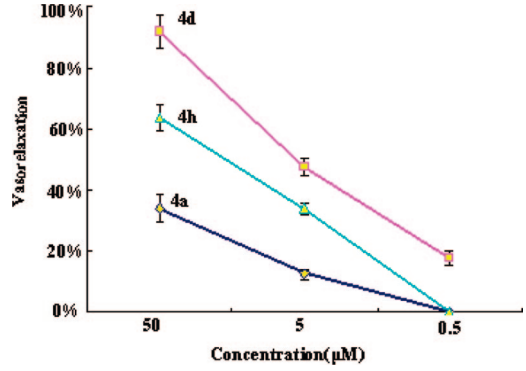

Figure 3. Vasorelaxation activities of **4a**,**d**,**h** at different concentrations.

be done. Furthermore, to really identify if PDE5 is the target, the enzyme inhibition studies are also worthwhile.

To understand the contribution of the imidazo ring to the vasorelaxation activities, **3a**−**q** were used as reference compounds, the vasorelaxation activities were tested using the same in vitro vasodilation model, and the data are also listed in Table 1. The data indicated that even increasing the final concentration by 100-fold **3a**−**q** exhibited weaker vasodilation. This comparison demonstrated that the imidazo ring had a great contribution to the vasorelaxation activity.

To explore the possible dose-dependent relaxation of **4a**−**q** the activities of 50, 5, and 0.5 μM of **4a**,**d**,**h** were evaluated on a NE constrict aortic strip and the results are shown in Figure 4. The data demonstrate that the activities of different dose **4a**,**d**,**h** are significantly different from each other and they exhibit dose-dependent vasorelaxation (Figure 3).

Alignment of 4a−**q.** Establishing the valid 3D-QSAR models a proper alignment procedure of **4a**−**q** was practiced using the target model align strategy in the align module within Cerius^2. On the basis of the assumption that each structure of **4a**−**q** exhibits activity at the same binding site of the receptor, they were aligned in a pharmacologically active orientation. To obtain a consistent alignment, the most vasorelaxation potent **4d** was selected as the template for superposing **4a**−**c**,**e**−**q**. The method

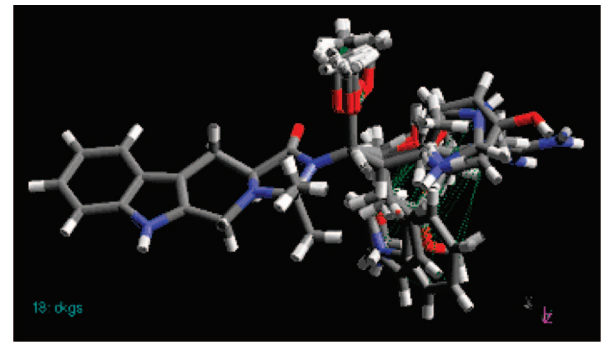

Figure 4. Alignment stereoview of **4a**−**q** used for molecular field generation.

used for performing the alignment was the maximum common subgraph (MCS).[21] MCS looks at molecules as points and lines and uses the techniques out of graph theory to identify the patterns. Then MCS finds the largest subset of atoms in **4d** that shared by **4a**−**c**,**e**−**q**. This subset was used for the alignment. A rigid fit of atom pairings was performed to superimpose each structure onto the target model **4d**. Stereoview of aligned **4a**−**q** is shown in Figure 4. The alignment stereoview explores that to superimpose onto **4d** the side chains of each structure has to take individual conformation. This individual side chain conformation will affect on the vasorelaxation activity.

QSAR module of Cerius^2 based MFA of 4a−**q.** Molecular field analysis (MFA) was performed for **4a**−**q** using the QSAR module of Cerius^2.[22] A five-step procedure consisted of generating conformers, energy minimization, matching atoms and aligning molecules, setting preferences, and regression analysis was automatically practiced in MFA. Molecular electrostatic and steric fields were created by use of proton and methyl groups as probes, respectively. These fields were sampled at each point of a regularly spaced grid of 1 Å. An energy cutoff of ± 30.0 kcal/mol was set for both electrostatic and steric fields. The total grid points generated were 672. Although the spatial and structural descriptors such as dipole moment, polarizability, radius of gyration, number of rotatable bonds, molecular volume, principal moment of intertia, AlogP98, number of hydrogen bond donors and acceptors, and molar refractivity were also considered, only the highest variance holder proton and methyl descriptors were used. Regression analysis was carried out using the genetic partial least-squares (G/PLS) method consisting of 50000 generations with a population size of 100. The number of components was set to 5. Cross-validation was performed with the leave-one-out procedure. PLS analysis was scaled, with all variables normalized to a variance of 1.0.

The regions where variations in the steric or electrostatic features of **4a**−**q** in the training set lead to increase or decrease activities were specified. Proton descriptor with positive coefficient indicates a region favorable for electropositive group, while negative coefficient indicates electronegative group required at the position. The MFA model for the activity of **4a**−**q** (Figure 5) in terms of the most relevant descriptors proton and methyl group is expressed by eq 1.

$$\begin{aligned}\text{Activity} = {} & 1.79841 - 0.049782(H^+/241) - \\ & 0.0181689(H^+/248) + 0.03947(H^+/138) - \\ & 0.045626(CH_3/137) - 0.042326(H^+/137) + \\ & 0.046705(CH_3/139) + 0.04427(CH_3/87) + \\ & 0.04753(H^+/199) - 0.040812(CH_3/264) \quad (1)\end{aligned}$$

The correlation of the activities tested on the in vitro vasodilation model and the activities calculated using eq 1 is

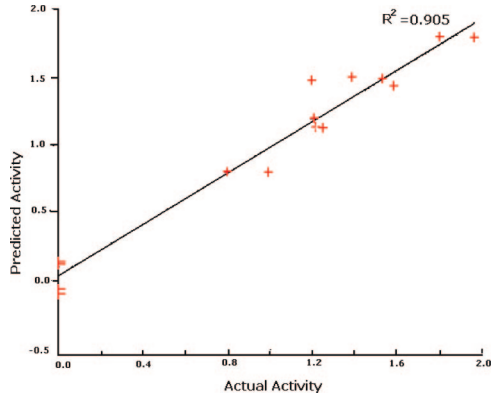

Figure 5. Graph of tested versus predicted activities of **4a**−**q**.

explained by Figure 6 (r^2, 0.905). In eq 1, the data points (n), correlation coefficient (r), square correlation coefficient (r^2), cross-validated correlation coefficient (r^2cv), bootstrap correlation coefficient (r^2BS), and least-squares error (LSE) were 17, 0.951, 0.905, 0.838, 0.616, and 0.045, respectively.

Equation 1 contains 5 terms from proton descriptor. Among them term 0.04753 (H^+/199) has the highest positive coefficient, which means that at this position an electron withdrawing group will affect on the activity negatively. Figure 7a gives two representatives, of which **4a** has no electron withdrawing group at this position and is vasorelaxation active, while **4n** has an electron withdrawing group at this position and is vasorelaxation inactive.

Equation 1 contains also 4 terms from methyl descriptor. Among them term (CH_3/137) and (CH_3/264) have negative coefficients, which means that at this position an hydrophobic group will affect on the activity negatively. Figure 6b gives two representatives, of which **4d** has no hydrophobic group at this position and is vasorelaxation active, while **4f** has an hydrophobic group at this position and is vasorelaxation nonactive.

Docking Studies on the Representatives of 4a−q. As mentioned above, the vasorelaxation activities of **4a**−**q** on a NE constrict aortic strip model are significantly different from each other and their structures are highly similar to tadalafil, a specific inhibitor of PDE5. Thus PDE5 was considered as one of the possible target enzymes of **4a**−**q** to evaluate their binding orientations and the interaction energies between PDE5 and them. Docking studies for **4a**−**q** were carried out using LigandFit module of Cerius2[23] and the crystal structure of PDE5 (PDB ID: 1XOZ). The active site of PDE5 was defined as a sphere of radius 6.0 A surrounding tadalafil.

Energetically, the most favorable conformation of the docked structure was selected on the basis of the LigandFit score and visual inspection. Initially hydrogen atoms were added to the protein, considering all the residues at their neutral form. Evaluation of the docking results was based on PDE5−**4a**−**q** complementarity, the steric and electrostatic properties, the calculated interaction energies in PDE5−**4a**−**q** complexes, and the intramolecular energies of **4a**−**q**. An evaluation was given to the adaptability of **4a**,**d**,**h** represented the vasorelaxation active compounds and **4f** represented the vasorelaxation inactive compounds to PDE5′s active site. Figure 7a demonstates that compound **4d** is suitable for sandwiching into PDE5′s hydrophobic clamp that contains hydrophobic amino acids Leu765, Val782, Phe786, Leu804, and Phe820 and forming an H bond with Tyr612. Figure 7b demonstates that compounds **4a**,**d**,**h** (shown in gray) are suitable for sandwiching into PDE5′s hydrophobic clamp consisted of hydrophobic amino acids Leu765, Val782, Phe786, Leu804, and Phe820 and forming an H bond with Tyr612. On the other hand, however, when **4f** sandwiches into PDE5′s hydrophobic clamp consisted of hydrophobic amino acids Leu765, Val782, Phe786, Leu804, and Phe820, the hydrophobic part of its tetracycle is more near the hydrophilic amino acids Gln775 and Gln817 of the pocket, which is unfavorable to the formation of the H bond. Besides, its side chain benzyl has an endo-orientation toward its tetracycle, which is unfavorable to sandwiching into PDE5′s hydrophobic clamp. The docking results are completely consistent with that of the crystal structures of **4f**,**h**.

Conclusion

Structural similarity of 17 novel methyl (11a*S*)-1,2,3,5,11,11a-hexahydro-3,3-dimethyl-1-oxo-6*H*-imidazo[3′,4′:1,2]pyridin[3,4-*b*]indol-2-substituted acetates (**4a**−**q**) to sildenafil, vardenafil, and tadalafil lends themselves the capacities of relaxing smooth muscle and blood vessel. Using docking study, we implied that PDE5 should be their target, and their capacities of relaxing smooth muscle and blood vessel essentially relied on their adaptability to the pocket of PDE5. For instance, the most potent **4d** is capable of sandwiching into PDE5′s hydrophobic clamp consisted of hydrophobic amino acids Leu765, Val782, Phe786, Leu804, and Phe820 and forming H bond with Tyr612, while the inactive **4f** is neither capable of sandwiching into this pocket nor capable of forming this H bond. We demonstrated that the conformations of **4f**,**h** from the docking, MFA, and crystal studies consistently reflected the importance of adapting the pocket of PDE5. These results should be useful for designing vasodilators with PDE5 as target.

Experimental Section

Synthesis. General. The protected amino acids with L-configuration were purchased from Sigma Chemical Co. All coupling and deprotective reactions were carried out under anhydrous conditions. Chromatography was performed on Qingdao silica gel H. The purities of the intermediates and the products were confirmed on thin layer chromatography (TLC, Merck silica gel plates of type 60 F_{254}, 0.25 mm layer thickness) and HPLC (Waters, C_{18} column 4.6 mm × 150 mm). ^{1}H NMR and ^{13}C NMR spectra were recorded on Bruker Advance 300 and 500 spectrometers. FAB-MS was determined by VG-ZAB-MS high resolution GC/MS/DS and HP ES-5989x. Optical rotations were determined with a Schmidt+Haensch Polartromic D instrument. The statistical analysis of all the biological date was carried out by use of ANOVA test with $p < 0.05$ as significant cutoff.

(*S*)-2,3,4,9-Tetrahydro-1*H*-pyrido[3,4-*b*]indole-3-carboxylic Acid (1).[24] Compound **1** was prepared according to the literature.

(*S*)-2-(*tert*-Butoxycarbonyl)-2,3,4,9-tetrahydro-1*H*-pyrido[3,4-*b*]indole-3-carboxylic Acid (2). Compound **2** was prepared according to the literature.

General Procedure for the Preparation of Substituted (*S*)-*tert*-Butyl 3-(2-Methoxy-2-oxoethylcarbamoyl)-3,4-dihydro-1*H*-pyrido[3,4-*b*]indole-2(9*H*)-carboxylate (3a−q). At 0 °C, to the solution of 2.0 g (6.33 mmol) (*S*)-2-(*tert*-butoxycarbonyl)-2,3,4,9-tetrahydro-1*H*-pyrido[3,4-*b*]indole-3-carboxylic acid in 30 mL of anhydrous tetrahydrofuran (THF), 1.2 g (8.9 mmol) of *N*-hydroxybenzotriazole (HOBt) were added; after 10 min, 1.75 g (8.5 mmol) of dicyclohexylcarbodiimide (DCC) were then added. The suspension of 6.61 mmol of HCl·L-AA-OMe in 3 mL of anhydrous THF was adjusted pH to 8−9 with *N*-methyl morpholine and stirred at room temperature for another 20 min. This suspension then was added to the solution of (*S*)-2-(*tert*-butoxycarbonyl)-2,3,4,9-tetrahydro-1*H*-pyrido[3,4-*b*]indole-3-carboxylic acid and the reaction mixture was stirred at 0 °C for 2 h and at room temperature for 16 h. On evaporation, the residue was dissolved in 30 mL of ethyl acetate. The solution was washed successively with 5% sodium

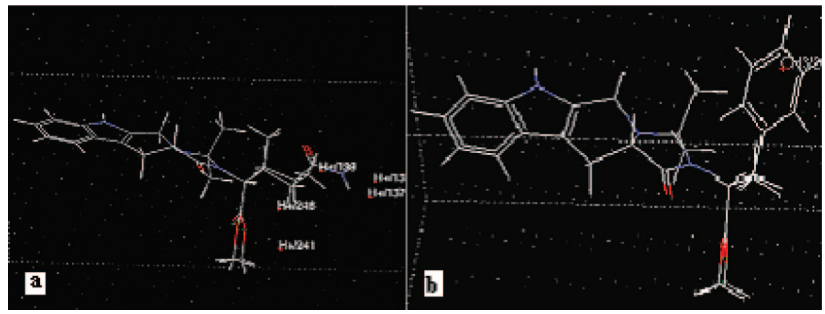

Figure 6. (a) Electrostatic environment of **4a**,**n** within the grid with 3D points of eq 1. (b) Steric environment of **4d**,**f** within the grid with 3D points of eq 1.

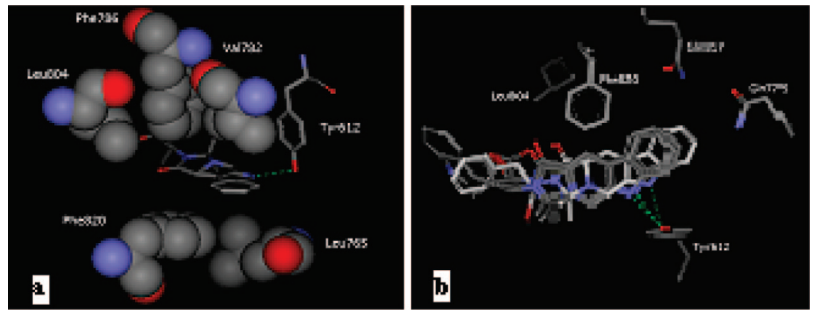

Figure 7. (a) Compound **4d** (shown in gray) sandwiching into the hydrophobic clamp and forming an H bond with Tyr612 of PDE5′s pocket. (b) Ensemble of **4a**,**d**,**h** (shown in gray) and **4f** (shown in white) sandwiching into PDE5′s pocket.

bicarbonate, 5% citric acid, and saturated sodium chloride, and the organic phase was separated and dried over anhydrous sodium sulfate. After filtration and evaporation under reduced pressure, the title compound were obtained as powder.

(*S*)-*tert*-Butyl 3-((2*S*)-1-Methoxy-3-methyl-1-oxopentan-2-ylcarbamoyl)-3,4-dihydro-1*H*-pyrido[3,4-*b*]indole-2(9*H*)-carboxylate (3a). Yield: 2.70 g (90%) as colorless powder; mp 122−125 °C. ESI/MS (*m*/*e*) 444 $[M + H]^+$. IR (KBr): 3445, 3203, 3006, 2953, 2842, 1727, 1644, 1607, 1452, 1394, 1372, 1062, 900 cm^{-1}. ^1H NMR (BHSC-500, DMSO-d_6): δ/ppm = 10.045 (s, 1H), 7.965 (s, 1H), 7.293 (t, J = 7.4 Hz, 1H), 7.214 (t, J = 7.4 Hz, 1H), 7.007 (d, J = 7.4 Hz, 1H), 6.895 (d, J = 7.4 Hz, 1H), 4.842 (t, J = 5.4 Hz,1H),4.425 (d, J = 5.4 Hz, 1H), 4.226 (dd, J = 10.2 Hz, J = 4.5 Hz, 1H), 4.039 (dd, J = 10.2 Hz, J = 3.7 Hz, 1H), 3.622 (s, 3H), 2.953 (d, J = 6.7 Hz, 2H), 2.877 (m, J = 6.0 Hz, 1H), 1.473 (s, 9H), 1.350 (m, J = 5.4 Hz, 2H), 1.053 (d, J = 5.4 Hz, 3H), 1.001 (t, J = 5.4 Hz, 3H). $[\alpha]_D^{20} = -49$ (c = 0.37, $CHCl_3$:CH_3OH, 1:1, v/v).

(*S*)-*tert*-Butyl 3-((*S*)-1-Methoxy-3-methyl-1-oxobutan-2-ylcarbamoyl)-3,4-dihydro-1*H*-pyrido[3,4-*b*]indole-2(9*H*)-carboxylate (3b). Yield: 2.65 g (97%) as colorless powder; mp 138−140 °C. ESI/MS (*m*/*e*) 430 $[M + H]^+$. IR (KBr): 3443, 3202, 3001, 2951, 2845, 1729, 1648, 1602, 1450, 1392, 1370, 1067, 902 cm^{-1}. ^1H NMR (BHSC-500, DMSO-d_6): δ/ppm = 10.043 (s, 1H), 7.962 (s, 1H), 7.295 (t, J = 7.4 Hz, 1H), 7.211 (t, J = 7.7 Hz, 1H), 7.004 (d, J = 7.7 Hz, 1H), 6.892 (d, J = 7.4 Hz, 1H), 4.840 (t, J = 5.4 Hz, 1H), 4.423 (d, J = 5.4 Hz, 1H), 4.225 (dd, J = 10.2 Hz, J = 4.5 Hz, 1H), 4.037 (dd, J = 10.2 Hz, J = 3.7 Hz, 1H), 3.626 (s, 3H), 3.103 (m, J = 5.4 Hz, 1H), 2.951 (d, J = 6.7 Hz, 2H), 1.474 (s, 9H), 1.053 (d, J = 5.4 Hz, 6H). $[\alpha]_D^{20} = -32$ (c = 0.30, $CHCl_3$:CH_3OH, 1:1, v/v).

(*S*)-*tert*-Butyl 3-((*S*)-1-Methoxy-4-methyl-1-oxopentan-2-ylcarbamoyl)-3,4-dihydro-1*H*-pyrido[3,4-*b*]indole-2(9*H*)-carboxylate (3c). Yield: 2.78 g (99%) as colorless powder; mp 131−133 °C. ESI/MS (*m*/*e*) 444 $[M + H]^+$. IR (KBr): 3443, 3205, 3002, 2954, 2845, 1724, 1642, 1605, 1455, 1392, 1370, 1065, 903 cm^{-1}. ^1H NMR (BHSC-500, DMSO-d_6): δ/ppm = 10.043 (s, 1H), 7.962 (s, 1H), 7.291 (t, J = 7.4 Hz, 1H), 7.212 (t, J = 7.4 Hz, 1H), 7.004 (d, J = 7.4 Hz, 1H), 6.891 (d, J = 7.4 Hz, 1H), 4.840 (t, J = 5.4 Hz, 1H), 4.422 (d, J = 5.4 Hz, 1H), 4.224 (dd, J = 10.2 Hz, J = 4.5 Hz, 1H), 4.036 (dd, J = 10.2 Hz, J = 3.7 Hz, 1H), 3.625 (s, 3H), 2.950 (d, J = 6.7 Hz, 2H), 1.877 (d, J = 6.0 Hz, 2H), 1.473 (s, 9H), 1.852 (m, J = 5.4 Hz, 1H), 1.055 (d, J = 5.4 Hz, 6H). $[\alpha]_D^{20} = -41$ (c = 0.31, $CHCl_3$:CH_3OH, 1:1, v/v).

(*S*)-*tert*-Butyl 3-((*S*)-1-Methoxy-1-oxopropan-2-ylcarbamoyl)-3,4-dihydro-1*H*-pyrido[3,4-*b*]indole-2(9*H*)-carboxylate (3d). Yield: 2.43 g (95.6%) as colorless powder; mp 144−146 °C. ESI/MS (*m*/*e*) 402 $[M + H]^+$. IR (KBr): 3451, 3011, 2949, 2847, 1730, 1604, 1450, 1392, 1370, 1066, 897 cm^{-1}. ^1H NMR (BHSC-500, DMSO-d_6): δ/ppm = 9.891 (s, 1H), 7.980 (s, 1H), 7.323 (t, J = 7.5 Hz, 1H), 7.235 (t, J = 7.8 Hz, 1H), 6.972 (d, J = 7.8 Hz, 1H), 6.813 (d, J = 7.5 Hz, 1H), 4.884 (d, J = 5.2 Hz, 1H), 4.591 (m, J = 5.5 Hz, 1H), 4.255 (dd, J = 10.0 Hz, J = 4.7 Hz, 1H), 4.172 (dd, J = 10.1 Hz, J = 3.5 Hz, 1H), 3.644 (s, 3H), 2.94 (d, J = 10.1 Hz, 2H), 1.556 (d, J = 5.2 Hz, 3H), 1.437 (s, 9H). $[\alpha]_D^{20} = -63$ (c = 0.35, $CHCl_3$:CH_3OH, 1:1, v/v).

(*S*)-*tert*-Butyl 3-(2-Methoxy-2-oxoethylcarbamoyl)-3,4-dihydro-1*H*-pyrido-[3,4-*b*]indole-2(9*H*)-carboxylate (3e). Yield: 2.39 g (97.6%) as colorless powder; mp 133−135 °C. ESI/MS (*m*/*e*) 388 $[M + H]^+$. IR (KBr): 3448, 3010, 2945, 2843, 1732, 1600, 1453, 1390, 1371, 1062, 899 cm^{-1}. ^1H NMR (BHSC-500, DMSO-d_6): δ/ppm = 9.934 (s, 1H), 8.025 (s, 1H), 7.302 (t, J = 7.5 Hz, 1H), 7.201 (t, J = 7.6 Hz, 1H), 6.955 (d, J = 7.6 Hz, 1H), 6.836 (d, J = 7.6 Hz, 1H), 4.891 (d, J = 5.4 Hz, 1H), 4.223 (dd, J = 10.2 Hz, J = 4.5 Hz, 1H), 4.182 (s, 2H), 4.194 (dd, J = 10.2 Hz, J = 3.7 Hz, 1H), 3.663 (s, 3H), 2.95 (d, J = 10.1 Hz, 2H), 1.455 (s, 9H). $[\alpha]_D^{20} = -101$ (c = 0.36, $CHCl_3$:CH_3OH, 1:1, v/v).

(*S*)-*tert*-Butyl 3-((*S*)-1-Methoxy-1-oxo-3-phenylpropan-2-ylcarbamoyl)-3,4-dihydro-1*H*-pyrido[3,4-*b*]indole-2(9*H*)-carboxylate (3f). Yield: 2.99 g (99.0%) as colorless powder; mp 150−152 °C. ESI/MS (*m*/*e*) 478 $[M + H]^+$. IR (KBr): 3446, 3205, 3006, 2948, 2847, 1731, 1645, 1603, 1451, 1392, 1370, 1069, 904 cm^{-1}. ^1H NMR (BHSC-500, DMSO-d_6): δ/ppm = 9.920 (s, 1H), 7.971 (s, 1H), 7.314 (t, J = 7.5 Hz, 1H), 7.282 (t, J = 7.9 Hz, 2H), 7.195 (t, J = 7.6 Hz, 1H), 7.140 (d, J = 7.6 Hz, 2H), 7.025 (t, J = 7.6 Hz, 1H), 6.963 (d, J = 7.8 Hz, 1H), 6.807 (d, J = 7.6 Hz, 1H), 4.935 (d, J = 5.4 Hz, 1H), 4.822 (t, J = 5.4 Hz, 1H), 4.274 (dd, J = 10.2 Hz, J = 4.5 Hz, 1H), 4.185 (dd, J = 10.2 Hz, J = 3.4 Hz,

1H), 3.625 (s, 3H), 3.17 (d, $J = 5.4$ Hz, 2H), 2.930 (d, $J = 10.2$ Hz, 2H), 1.483 (s, 9H). $[\alpha]_D^{20} = -64$ ($c = 0.36$, $CHCl_3$:CH_3OH, 1:1, v/v).

(*S*)-*tert*-Butyl 3-((*S*)-3-(4-Hydroxyphenyl)-1-methoxy-1-oxopropan-2-ylcarbamoyl)-3,4-dihydro-1*H*-pyrido[3,4-*b*]indole-2(9*H*)-carboxylate (3g). Yield: 2.87 g (92%) as colorless powder; mp 143−145 °C. ESI/MS (*m*/*e*) 494 $[M + H]^+$. IR (KBr): 3439, 3203, 3001, 2955, 2847, 1732, 1644, 1601, 1453, 1391, 1372, 1062, 903 cm^{-1}. ^1H NMR (BHSC-500, DMSO-d_6): δ/ppm = 9.990 (s, 1H), 8.024 (s, 1H), 7.371 (t, $J = 7.6$ Hz, 1H), 7.223 (t, $J = 7.7$ Hz, 1H), 7.152 (d, $J = 7.5$ Hz, 2H), 7.024 (d, $J = 7.5$ Hz, 1H), 6.961 (d, $J = 7.7$ Hz, 1H), 6.915 (d, $J = 7.5$ Hz, 2H), 4.980 (s, 1H), 4.935 (d, $J = 5.4$ Hz, 1H), 4.806 (t, $J = 5.6$ Hz, 1H), 4.292 (m, $J = 5.2$ Hz, 2H), 3.643 (s, 3H), 3.157 (d, $J = 5.2$ Hz, 2H), 2.975 (d, $J = 5.0$ Hz, 2H), 1.49 3 (s, 9H). $[\alpha]_D^{20} = -57$ ($c = 0.32$, $CHCl_3$:CH_3OH, 1:1, v/v).

(*S*)-*tert*-Butyl 3-((*S*)-3-(1*H*-Indol-3-yl)-1-methoxy-1-oxopropan-2-ylcarbamoyl)-3,4-dihydro-1*H*-pyrido[3,4-b]indole-2(9*H*)-carboxylate (3h). Yield: 2.78 g (85%) as colorless powder; mp 161−163 °C. ESI/MS (*m*/*e*) 517 $[M + H]^+$. IR (KBr): 3442, 3204, 3000, 2948, 2839, 1729, 1642, 1604, 1448, 1391, 1372, 1062, 900 cm^{-1}. H NMR (BHSC-500, DMSO-d_6): δ/ppm = 9.872 (s, 1H), 9.863 (s, 1H), 8.095 (s, 1H), 7.324 (t, $J = 7.5$ Hz, 1H), 7.307 (t, $J = 7.4$ Hz, 1H), 7.126 (d, $J = 7.8$ Hz, 1H), 7.114 (t, $J = 7.8$ Hz, 1H), 7.103 (d, $J = 7.6$ Hz, 1H), 7.095 (t, $J = 7.8$ Hz, 1H), 7.046 (d, $J = 7.6$ Hz, 1H), 6.981 (d, $J = 7.5$ Hz, 1H), 6.835 (s, 1H), 4.94 (d, $J = 5.4$ Hz, 1H), 4.762 (t, $J = 5.3$ Hz, 1H), 4.291 (d, $J = 5.2$ Hz, 2H), 3.644 (s, 3H), 3.192 (d, $J = 5.4$ Hz, 2H), 2.955 (d, $J = 6.4$ Hz, 2H), 1.496 (s, 9H). $[\alpha]_D^{20} = -79$ ($c = 0.34$, $CHCl_3$:CH_3OH, 1:1, v/v).

(*S*)-Dimethyl 2-((*S*)-2-(*tert*-Butoxycarbonyl)-2,3,4,9-tetrahydro-1*H*-pyrido[3,4-*b*]-indole-3-carboxamido)succinate (3i). Yield: 2.79 g (96%) as colorless powder; mp 158−160 °C. ESI/MS (*m*/*e*) 460 $[M + H]^+$. IR (KBr): 3441, 3210, 3004, 2955, 2841, 1732, 1643, 1604, 1453, 1390, 1371, 1061, 903 cm^{-1}. ^1H NMR (BHSC-500, DMSO-d_6): δ/ppm = 10.050 (s, 1H), 8.051 (s, 1H), 7.373 (t, $J = 7.4$ Hz, 1H), 7.252 (t, $J = 7.4$ Hz, 1H), 7.006 (d, $J = 7.6$ Hz, 1H), 6.954 (d, $J = 7.4$ Hz, 1H), 4.926 (d, $J = 5.5$ Hz, 1H), 4.773 (t, $J = 5.5$ Hz, 1H), 4.242 (d, $J = 5.6$ Hz, 2H), 3.625 (s, 3H), 3.581 (s, 3H), 2.917 (d, $J = 5.2$ Hz, 2H), 2.855 (d, $J = 5.4$ Hz, 2H), 1.494 (s, 9H). $[\alpha]_D^{20} = -52$ ($c = 0.35$, $CHCl_3$:CH_3OH, 1:1, v/v).

(*S*)-Dimethyl 2-((*S*)-2-(*tert*-Butoxycarbonyl)-2,3,4,9-tetrahydro-1*H*-pyrido[3,4-*b*]-indole-3-carboxamido)pentanedioate (3j). Yield: 2.93 g (98%) as colorless powder; mp 154−156 °C. ESI/MS (*m*/*e*) 474 $[M + H]^+$. IR (KBr): 3441, 3203, 3000, 2944, 2831, 1731, 1645, 1604, 1455, 1390, 1372, 1067, 903 cm^{-1}. ^1H NMR (BHSC-500, DMSO-d_6): δ/ppm = 9.890 (s, 1H), 8.044 (s, 1H), 7.393 (t, $J = 7.6$ Hz, 1H), 7.282 (t, $J = 7.6$ Hz, 1H), 7.015 (d, $J = 7.7$ Hz, 1H), 6.844 (d, $J = 7.6$ Hz, 1H), 4.906 (d, $J = 5.4$ Hz, 1H), 4.437 (t, $J = 5.6$ Hz, 1H), 4.225 (d, $J = 5.5$ Hz, 2H), 3.663 (s, 3H), 3.647 (s, 3H), 2.968 (d, $J = 5.4$ Hz, 2H), 2.281 (t, $J = 5.6$ Hz, 2H), 2.245 (t, $J = 5.7$ Hz, 2H), 1.434 (s, 9H). $[\alpha]_D^{20} = -45$ ($c = 0.37$, $CHCl_3$:CH_3OH, 1:1, v/v).

(*S*)-*tert*-Butyl 3-((*S*)-3-hydroxy-1-methoxy-1-oxopropan-2-ylcarbamoyl)-3,4-dihydro-1*H*-pyrido[3,4-*b*]indole-2(9*H*)-carboxylate (3k). Yield: 2.43 g (92%) as colorless powder; mp 139−141 °C. ESI/MS (*m*/*e*) 418 $[M + H]^+$. IR (KBr): 3442, 3200, 3001, 2952, 2845, 1730, 1644, 1606, 1455, 1392, 1370, 1067, 900 cm^{-1}. ^1H NMR (BHSC-500, DMSO-d_6): δ/ppm = 9.950 (s, 1H), 7.972 (s, 1H), 7.291 (t, $J = 7.6$ Hz, 1H), 7.224 (t, $J = 7.9$ Hz, 1H), 6.995 (d, $J = 7.9$ Hz, 1H), 6.830 (t, $J = 7.6$ Hz, 1H), 4.872 (d, $J = 5.4$ Hz, 1H), 4.526 (t, $J = 5.6$ Hz, 1H), 4.197 (d, $J = 5.2$ Hz, 2H), 4.133 (d, $J = 5.6$ Hz, 2H), 3.634 (s, 3H), 2.95 (d, $J = 5.6$ Hz, 1H), 2.925 (d, $J = 5.6$ Hz, 1H), 2.288 (s, 1H), 1.454 (s, 9H). $[\alpha]_D^{20} = -57$ ($c = 0.38$, $CHCl_3$:CH_3OH, 1:1, v/v).

(*S*)-*tert*-Butyl 3-((2*S*)-3-Hydroxy-1-methoxy-1-oxobutan-2-ylcarbamoyl)-3,4-dihydro-1*H*-pyrido[3,4-*b*]indole-2(9*H*)-carboxylate (3l). Yield: 2.37 g (87%) as colorless powder; mp 140−142 °C. ESI/MS (*m*/*e*) 432 $[M + H]^+$. IR (KBr): 3437, 3200, 3002, 2951, 2844, 1735, 1649, 1600, 1450, 1392, 1370, 1065, 901 cm^{-1}. ^1H NMR (BHSC-500, DMSO-d_6): δ/ppm = 9.981 (s, 1H), 7.870 (s, 1H), 7.343 (t, $J = 7.4$ Hz, 1H), 7.254 (t, $J = 7.6$ Hz, 1H), 6.952 (d, $J = 7.6$ Hz, 1H), 6.724 (d, $J = 7.4$ Hz, 1H), 4.870 (t, $J = 5.4$ Hz, 1H), 4.673 (m, $J = 5.6$ Hz, 1H), 4.485 (t, $J = 5.6$ Hz, 1H), 3.991 (m, $J = 5.2$ Hz, 2H), 3.653 (s, 3H), 2.974 (d, $J = 5.7$ Hz, 2H), 2.195 (d, $J = 3.7$ Hz, 1H), 1.474 (s, 9H), 1.19(d, $J = 5.6$ Hz, 3H). $[\alpha]_D^{20} = -65$ ($c = 0.35$, $CHCl_3$:CH_3OH, 1:1, v/v).

(*S*)-*tert*-Butyl 3-((*S*)-4-Amino-1-methoxy-1,4-dioxobutan-2-ylcarbamoyl)-3,4-dihydro-1*H*-pyrido[3,4-*b*]indole-2(9*H*)-carboxylate (3m). Yield: 2.13 g (76%) as colorless powder; mp 127−129 °C. ESI/MS (*m*/*e*) 445 $[M + H]^+$. IR (KBr): 3440, 3203, 3005, 2942, 2833, 1735, 1642, 1604, 1453, 1394, 1372, 1067, 903 cm^{-1}. ^1H NMR (BHSC-500, DMSO-d_6): δ/ppm = 8.871 (s, 1H), 8.012 (s, 1H), 7.296 (t, $J = 7.4$ Hz, 1H), 7.217 (t, $J = 7.4$ Hz, 1H), 7.008 (d, $J = 7.4$ Hz, 1H), 6.827 (d, $J = 7.4$ Hz, 1H), 6.053 (s, 2H), 4.927 (d, $J = 5.5$ Hz, 1H), 4.422 (t, $J = 5.5$ Hz, 1H), 4.246 (d, $J = 5.6$ Hz, 2H), 3.674 (s, 3H), 2.942 (d, $J = 5.4$ Hz, 2H), 2.688 (t, $J = 5.5$ Hz, 2H), 1.466 (s, 9H). $[\alpha]_D^{20} = -51$ ($c = 0.38$, $CHCl_3$:CH_3OH, 1:1, v/v).

(*S*)-*tert*-Butyl 3-((*S*)-5-Amino-1-methoxy-1,5-dioxopentan-2-ylcarbamoyl)-3,4-dihydro-1*H*-pyrido[3,4-*b*]indole-2(9*H*)-carboxylate (3n). Yield: 2.38 g (82%) as colorless powder; mp 122−124 °C. ESI/MS (*m*/*e*) 459 $[M + H]^+$. IR (KBr): 3445, 3200, 3001, 2940, 2835, 1733, 1640, 1602, 1452, 1391, 1370, 1065, 900 cm^{-1}. ^1H NMR (BHSC-500, DMSO-d_6): δ/ppm = 9.916 (s, 1H), 8.007 (s, 1H), 7.292 (t, $J = 7.4$ Hz, 1H), 7.203 (t, $J = 7.4$ Hz, 1H), 7.005 (d, $J = 7.4$ Hz, 1H), 6.806 (d, $J = 7.4$ Hz, 1H), 6.054 (s, 2H), 4.925 (d, $J = 5.5$ Hz, 1H), 4.413 (t, $J = 5.5$ Hz, 1H), 4.245 (d, $J = 5.6$ Hz, 2H), 3.677 (s, 3H), 2.945 (d, $J = 5.4$ Hz, 2H), 2.186 (t, $J = 5.5$ Hz, 2H), 2.140 (t, $J = 5.5$ Hz, 2H), 1.464 (s, 9H). $[\alpha]_D^{20} = -56$ ($c = 0.38$, $CHCl_3$:CH_3OH, 1:1, v/v).

(*S*)-*tert*-Butyl 3-((*S*)-5-Guanidino-1-methoxy-1-oxopentan-2-ylcarbamoyl)-3,4-dihydro-1*H*-pyrido[3,4-*b*]indole-2(9*H*)-carboxylate (3o). Yield: 2.43 g (79%) as colorless powder; mp 168−170 °C. ESI/MS (*m*/*e*) 487 $[M + H]^+$. IR (KBr): 3443, 3207, 3001, 2948, 2842, 1731, 1645, 1602, 1453, 1390, 1372, 1061, 904 cm^{-1}. ^1H NMR (BHSC-500, DMSO-d_6): δ/ppm = 10.221 (s, 1H), 8.452 (s, 2H), 8.270 (s, 1H), 8.224 (s, 1H), 8.017 (s, 1H), 7.293 (t, $J = 7.6$ Hz, 1H), 7.185 (t, $J = 7.7$ Hz, 1H), 7.044 (d, $J = 7.7$ Hz, 1H), 6.961 (d, $J = 7.6$ Hz, 1H), 4.905 (d, $J = 5.3$ Hz, 1H), 4.426 (t, $J = 4.2$ Hz, 1H), 4.251 (d, $J = 5.0$ Hz, 2H), 3.655 (s, 3H), 2.947 (d, $J = 4.1$ Hz, 2H), 2.680 (t, $J = 5.4$ Hz, 2H), 1.925 (m, $J = 5.5$ Hz, 2H), 1.583 (m, $J = 5.5$ Hz, 2H), 1.576 (s, 9H). $[\alpha]_D^{20} = -45$ ($c = 0.35$, $CHCl_3$:CH_3OH, 1:1, v/v).

(*S*)-*tert*-Butyl 3-((*S*)-3-(1*H*-Imidazol-4-yl)-1-methoxy-1-oxopropan-2-ylcarbamoyl)-3,4-dihydro-1*H*-pyrido[3,4-*b*]indole-2(9*H*)-carboxylate (3p). Yield: 2.36 g (80%) as colorless powder; mp 162−164 °C. ESI/MS (*m*/*e*) 468 $[M + H]^+$. IR (KBr): 3442, 3206, 3004, 2949, 2839, 1730, 1643, 1601, 1454, 1391, 1368, 1062, 902 cm^{-1}. ^1H NMR (BHSC-500, DMSO-d_6): δ/ppm = 12.980 (s, 1H), 9.962 (s, 1H), 8.053 (s, 1H), 7.475 (s, 1H), 6.85 (s, 1H), 7.362 (t, $J = 7.4$ Hz, 1H), 7.206 (t, $J = 7.7$ Hz, 1H), 7.164 (d, $J = 7.7$ Hz, 1H), 6.985 (t, $J = 7.4$ Hz, 1H), 4.937 (t, $J = 5.3$ Hz, 1H), 4.835 (t, $J = 5.4$ Hz, 1H), 4.266 (d, $J = 5.2$ Hz, 2H), 3.645 (s, 3H), 3.194 (d, $J = 5.4$ Hz, 2H), 2.925 (d, $J = 5.2$ Hz, 2H), 1.493 (s, 9H). $[\alpha]_D^{20} = -47$ ($c = 0.30$, $CHCl_3$:CH_3OH, 1:1, v/v).

(*S*)-*tert*-Butyl 3-((*S*)-1-Methoxy-4-(methylthio)-1-oxobutan-2-ylcarbamoyl)-3,4-dihydro-1*H*-pyrido[3,4-*b*]indole-2(9*H*)-carboxylate (3q). Yield: 2.80 g (97%) as colorless powder; mp 159−161 °C. ESI/MS (*m*/*e*) 462 $[M + H]^+$. IR (KBr): 3441, 3203, 3004, 2953, 2847, 1732, 1641, 1603, 1454, 1390, 1372, 1061, 900 cm^{-1}. ^1H NMR (BHSC-500, DMSO-d_6): δ/ppm = 10.04 (s, 1H), 7.97 (s, 1H), 7.32 (t, $J = 7.5$ Hz, 1H), 7.22 (t, $J = 7.8$ Hz, 1H), 6.99 (d, $J = 7.8$ Hz, 1H), 6.81 (d, $J = 7.5$ Hz, 1H), 4.86 (t, $J = 5.3$ Hz, 1H), 4.45 (t, $J = 5.5$ Hz, 1H), 4.28 (d, $J = 5.1$ Hz, 2H), 3.68 (s, 3H), 2.93 (d, $J = 5.3$ Hz, 2H), 2.42 (t, $J = 5.4$ Hz, 2H), 2.28

(d, J = 5.6 Hz, 2H), 2.10 (s, 3H), 1.44 (s, 9H). $[\alpha]_D^{20} = -48$ (c = 0.33, $CHCl_3$:CH_3OH, 1:1, v/v).

General Procedure for the Preparation of Methyl (11a*S*)-1,2,3,5,11,11a- hexahydro-3,3-dimethyl-1-oxo-6*H*-imidazo[3′,4′:1,2]pyridin[3,4-*b*]indol-2-substituted Acetate (4a−q). At 0 °C to the solution of 4.51 mmol of substituted (*S*)-*tert*-butyl 3-(2-methoxy-2-oxoethylcarbamoyl)-3,4-dihydro-1*H*-pyrido[3,4-*b*]indole-2(9*H*)-carboxylate (**3**) in 8 mL of ethyl acetate 16 mL of hydrogen chloride/ethyl acetate (4N) were added dropwise. The reaction solution was stirred at 0 °C for 90min and evaporated under reduced pressure. The residue was dissolved in 60 mL of methanol and 20 mL of acetone. The reaction solution was adjusted to pH 9 with triethylamine, stirred at room temperature and in dark for 240 h, and TLC ($CHCl_3$/MeOH, 10/1) indicated the complete disappearance of **3**. On evaporation, the residue was dissolved in 200 mL of ethyl acetate. The solution was washed successively with 5% sodium bicarbonate, 5% citric acid, and saturated sodium chloride, and the organic phase was separated and dried over anhydrous sodium sulfate. After filtration and evaporation under reduced pressure, the residues of **4a**−**l**,**n**,**q** were dissolved in 5 mL of methanol to purify via direct crystallization, while the residues of **4m**,**o**,**p** were purified on silica column chromatography ($CHCl_3$/CH_3OH, 10:1).

Methyl (11a*S*)-1,2,3,5,11,11a-Hexahydro-3,3-dimethyl-1-oxo-6*H*-imidazo-[3′,4′:1,2]pyridin[3,4-*b*]indol-2-(2′*S*, 3′*S*)-but-2-ylacetate (4a). Yield: 0.8 g (46%) as yellowish crystals. ESI/MS (*m*/*e*) 384 $[M + H]^+$. ^{1}H NMR ($CDCl_3$, 300 MHz) δ/ppm = 8.100 (s, 1H), 7.425 (t, J = 7.5 Hz, 1H), 7.252 (t, J = 7.5 Hz, 1H), 7.093 (d, J = 7.5 Hz, 1H), 7.060 (d, J = 7.5 Hz, 1H), 4.391 (t, J = 6.6 Hz, 1H), 3.914 (t, J = 6.6 Hz, 1H), 3.763 (dd, J = 10.5 Hz, J = 4.2 Hz, 2H), 3.666 (s, 3H), 2.931 (m, J = 6.2 Hz, 1H), 2.725 (d, J = 6.6 Hz, 2H), 1.489 (m, J = 6.0 Hz, 2H), 1.440 (s, 3H), 1.209 (s, 3H), 0.922 (d, J = 6.6 Hz, 3H), 0.853 (t, J = 6.6 Hz, 3H). ^{13}C NMR ($CDCl_3$, 75 MHz) δ/ppm = 171.911, 171.243, 136.257, 131.082, 127.109, 121.612, 119.519, 118.076, 110.749, 108.013, 78.953, 60.665, 57.410, 52.135, 41.569, 33.937, 25.457, 24.929, 23.883, 18.657, 16.391, 11.207. $[\alpha]_D^{20} = -94$ (c = 0.26, acetone).

Methyl (11a*S*)-1,2,3,5,11,11a-Hexahydro-3,3-dimethyl-1-oxo-6*H*-imidazo-[3′,4′:1,2]pyridin[3,4-*b*] indol-2-(2′*S*)-isopropylacetate (4b). Yield: 0.96 g (56%) as colorless powder. ESI/MS (*m*/*e*) 370 $[M + H]^+$. ^{1}H NMR ($CDCl_3$, 300 MHz) δ/ppm = 8.251 (s, 1H), 7.503 (t, J = 7.5 Hz, 1H), 7.313 (t, J = 7.5 Hz, 1H), 7.127 (d, J = 7.5 Hz, 1H), 7.102 (d, J = 7.5 Hz, 1H), 3.981 (d, J = 6.5 Hz, 1H), 3.844 (t, J = 5.5 Hz, 1H), 3.735 (s, 3H), 3.477 (dd, J = 4.5 Hz, J = 10.8 Hz, 1H), 3.194 (dd, J = 4.5 Hz, J = 10.8 Hz, 1H), 2.951 (m, J = 5.5 Hz, 1H), 2.726 (d, J = 5.5 Hz, 2H), 1.505 (s, 3H), 1.442 (s, 3H), 1.206 (m, J = 6.6 Hz, 3H), 0.999 (m, J = 6.6 Hz, 3H). ^{13}C NMR ($CDCl_3$, 75 MHz): δ/ppm = 172.637, 170.185, 136.249, 130.974, 127.175, 121.736, 119.650, 118.183, 110.700, 108.326, 78.846, 61.728, 57.393, 52.193, 41.652, 33.937, 27.773, 23.899, 20.504, 19.828, 18.814. $[\alpha]_D^{20} = -105$ (c = 0.22, acetone).

Methyl (11a*S*)-1,2,3,5,11,11a-Hexahydro-3,3-dimethyl-1-oxo-6*H*-imidazo-[3′,4′:1,2]pyridin[3,4-*b*]indol-2-(2′*S*)-isobutylacetate (4c). Yield: 1.14 g (65%) as colorless powder; mp 204−206 °C. ESI/MS (*m*/*e*) 384 $[M + H]^+$. ^{1}H NMR ($CDCl_3$, 300 MHz) δ/ppm = 8.503 (s, 1H), 7.434 (t, J = 7.2 Hz, 1H), 7.254 (d, J = 7.2 Hz, 1H), 7.064 (d, J = 7.2 Hz, 1H), 7.007 (d, J = 7.2 Hz, 1H), 4.438 (t, J = 4.9 Hz, 1H), 3.997 (t, J = 5.2 Hz, 1H), 3.664 (s, 3H), 3.430 (dd, J = 4.2 Hz, J = 10.5 Hz, 1H), 3.089 (dd, J = 4.2 Hz, J = 10.5 Hz, 1H), 2.734 (d, J = 5.2 Hz, 2H), 2.189 (m, J = 4.9 Hz, 2H), 1.888 (m, J = 4.9 Hz, 1H), 1.432 (s, 3H), 1.273 (s, 3H), 0.921 (d, J = 4.9 Hz, 6H). ^{13}C NMR ($CDCl_3$, 75 MHz) δ/ppm = 171.647, 171.342, 136.266, 131.123, 127.159, 121.637, 119.535, 118.093, 110.758, 108.087, 78.475, 57.360, 52.852, 52.465, 41.668, 39.064, 25.210, 25.061, 23.611, 22.473, 22.374, 19.787. $[\alpha]_D^{20} = -89$ (c = 0.25, acetone).

Methyl (11a*S*)-1,2,3,5,11,11a-Hexahydro-3,3-dimethyl-1-oxo-6*H*-imidazo-[3′,4′:1,2]pyridin[3,4-*b*]indol-2-(2′*S*)-methylacetate (4d). Yield: 0.69 g (41%) as colorless powder. ESI/MS (*m*/*e*) 342 $[M + H]^+$. ^{1}H NMR ($CDCl_3$, 300 MHz) δ/ppm = 8.328 (s, 1H), 7.437 (t, J = 7.2 Hz, 1H), 7.256 (d, J = 7.2 Hz, 1H), 7.053 (d, J = 7.2 Hz, 1H), 7.000 (d, J = 7.2 Hz, 1H), 4.431 (t, J = 4.8 Hz, 1H), 3.990 (t, J = 5.4 Hz, 1H), 3.660 (s, 3H), 3.423 (dd, J = 4.3 Hz, J = 10.0 Hz, 1H), 3.088 (dd, J = 4.3 Hz, J = 10.0 Hz, 1H), 2.741 (d, J = 5.4 Hz, 2H), 1.490 (d, J = 4.8 Hz, 3H), 1.433 (s, 3H), 1.271 (s, 3H). ^{13}C NMR ($CDCl_3$, 75 MHz) δ/ppm = 173.555, 170.811, 136.706, 131.442, 127.725, 122.304, 120.113, 118.905, 111.202, 108.890, 70.879, 60.131, 51.011, 44.551, 42.107, 30.113, 29.107, 25.004, 14.115. $[\alpha]_D^{20} = -87$ (c = 0.28, acetone).

Methyl (11a*S*)-1,2,3,5,11,11a-Hexahydro-3,3-dimethyl-1-oxo-6*H*-imidazo-[3′,4′:1,2]pyridin[3,4-*b*]indol-2-acetate (4e). Yield: 0.76 g (45%) as colorless powder. ESI/MS (*m*/*e*) 329 $[M + H]^+$. ^{1}H NMR ($CDCl_3$, 300 MHz) δ/ppm = 8.522 (s, 1H), 7.439 (t, J = 7.4 Hz, 1H), 7.260 (d, J = 7.4 Hz, 1H), 7.058 (d, J = 7.4 Hz, 1H), 7.007 (d, J = 7.4 Hz, 1H), 4.335 (s, 2H), 3.977 (t, J = 5.6 Hz, 1H), 3.662 (s, 3H), 3.431 (dd, J = 4.1 Hz, J = 10.2 Hz, 1H), 3.092 (dd, J = 4.1 Hz, J = 10.2 Hz, 1H), 2.744 (d, J = 5.6 Hz, 2H), 1.430 (s, 3H), 1.276 (s, 3H). ^{13}C NMR ($CDCl_3$, 75 MHz) δ/ppm = 172.167, 170.825, 136.651, 131.224, 124.333, 121.922, 120.400, 119.113, 111.363, 109.223, 71.112, 61.166, 50.958, 44.551, 42.867, 30.200, 29.535, 25.531. $[\alpha]_D^{20} = -74$ (c = 0.30, acetone).

Methyl (11a*S*)-1,2,3,5,11,11a-Hexahydro-3,3-dimethyl-1-oxo-6*H*-imidazo-[3′,4′:1,2]pyridin[3,4-*b*]indol-2-(2′*S*)-benzylacetate (4f). Yield: 0.98 g (45%) as colorless powder. ESI/MS (*m*/*e*) 418 $[M + H]^+$. ^{1}H NMR ($CDCl_3$, 300 MHz) δ/ppm = 8.807 (s, 1H), 7.416 (t, J = 7.2 Hz, 1H), 7.271 (t, J = 7.5 Hz, 2H), 7.259 (d, J = 7.2 Hz, 1H), 7.144 (d, J = 7.5 Hz, 2H), 7.079 (t, J = 7.5 Hz, 1H), 7.058 (d, J = 7.2 Hz, 1H), 7.006 (d, J = 7.2 Hz, 1H), 4.988 (t, J = 4.5 Hz, 1H), 4.372 (dd, J = 4.5 Hz, J = 10.5 Hz, 1H,), 3.689 (s, 3H), 3.564 (d, J = 4.5 Hz, 2H), 3.275 (d, J = 5.5 Hz, 2H), 2.910 (d, J = 4.5 Hz, 2H), 1.281 (s, 3H), 1.344 (s, 3H). ^{13}C NMR (DMSO-d_6, 75 MHz) δ/ppm = 171.144, 170.443, 138.284, 136.042, 135.886, 132.540, 132.391, 129.804, 128.279, 126.606, 120.548, 118.422, 112.551, 105.754, 77.955, 56.766, 56.049, 52.299, 41.198, 33.789, 24.319, 23.346, 22.882. $[\alpha]_D^{20} = -152$ (c = 0.25, acetone).

Methyl (11a*S*)-1,2,3,5,11,11a-Hexahydro-3,3-dimethyl-1-oxo-6*H*-imidazo-[3′,4′:1,2]pyridin[3,4-*b*]indol-2-(2′S)-(*p*-hydroxylbenzyl)acetate (4g). Yield: 0.76 g (43%) as colorless powder; mp 212−214 °C. ESI/MS (*m*/*e*) 434 $[M + H]^+$. ^{1}H NMR ($CDCl_3$, 300 MHz) δ/ppm = 8.792 (s, 1H), 7.405 (t, J = 7.2 Hz,1H), 7.272 (t, J = 7.2 Hz,1H), 7.257 (t, J = 7.5 Hz, 2H), 7.149 (d, J = 7.5 Hz, 2H), 7.056 (d, J = 7.2 Hz, 1H), 7.017 (d, J = 7.2 Hz, 1H), 5.638 (s, 1H), 4.800 (dd, J = 4.8 Hz, J = 10.8 Hz, 1H), 3.823 (t, J = 5.8 Hz, 1H), 3.664 (s, 3H), 3.661 (d, J = 5.8 Hz, 2H), 3.237 (d, J = 4.8 Hz, 2H), 2.890 (d, J = 5.8 Hz, 2H), 1.433 (t, 3H), 1.268 (s, 3H). ^{13}C NMR (DMSO-d_6, 75 MHz) δ/ppm = 171.003, 170.534, 155.987, 136.034, 132.573, 130.710, 128.271, 126.688, 120.540, 118.414, 117.466, 115.035, 110.897, 105.804, 78.021, 56.807, 56.321, 52.217, 41.255, 30.681, 24.841, 23.355, 17.989. $[\alpha]_D^{20} = -143$ (c = 0.26, acetone).

Methyl (11a*S*)-1,2,3,5,11,11a-Hexahydro-3,3-dimethyl-1-oxo-6*H*-imidazo-[3′,4′:1,2]pyridin[3,4-*b*]indol-2-(2′*S*)-(indole-3-yl-methyl)acetate (4h). Yield: 0.80 g (45%) as colorless powder; mp 204−206 °C. ESI/MS (*m*/*e*) 457 $[M + H]^+$. ^{1}H NMR ($CDCl_3$, 300 MHz) δ/ppm = 8.862 (s, 1H), 8.775 (s, 1H), 7.567 (t, J = 7.8 Hz, 1H), 7.415 (t, J = 7.8 Hz, 1H), 7.325 (t, J = 7.8 Hz, 1H), 7.268 (t, J = 7.8 Hz, 1H), 7.262 (d, J = 7.8 Hz, 1H), 7.247 (t, J = 7.8 Hz, 1H), 7.022 (d, J = 7.8 Hz, 1H), 7.010 (d, J = 7.8 Hz, 1H), 6.779 (s, 1H), 4.691 (dd, J = 4.5 Hz, J = 9.9 Hz, 1H), 3.781 (t, J = 4.7 Hz, 1H), 3.694 (s, 3H), 3.480 (m, J = 4.0 Hz, 2H), 3.199 (d, J = 4.5 Hz, 2H), 2.911 (d, J = 4.7 Hz, 2H), 1.500 (s, 3H), 1.232 (s, 3H). ^{13}C NMR (DMSO-d_6, 75 MHz) δ/ppm = 170.855, 170.641, 136.034, 135.985, 132.532, 132.383, 127.595, 126.663, 124.389, 120.894, 120.556, 118.447, 118.002, 117.482, 111.400, 110.864, 110.551, 105.787, 77.972, 56.882, 56.654, 52.217, 41.223, 27.690, 24.434, 23.750, 23.363. $[\alpha]_D^{20} = -128$ (c = 0.25, acetone).

Dimethyl (11a*S*)-1,2,3,5,11,11a-hexahydro-3,3-dimethyl-1-oxo-6*H*-imidazo-[3′,4′:1,2]pyridin[3,4-*b*]indol-2-(2′*S*)-succinate (4i). Yield: 0.97 g (56%) as colorless powder; mp 234−236 °C. ESI/MS (*m*/*e*) 400 $[M + H]^+$. ^{1}H NMR ($CDCl_3$, 300 MHz) δ/ppm

= 8.782 (s, 1H), 7.411 (t, J = 7.5 Hz, 1H), 7.301 (t, J = 7.5 Hz, 1H), 7.007 (d, J = 7.5 Hz, 1H), 6.995 (d, J = 7.5 Hz, 1H), 4.439 (t, J = 4.5 Hz, 1H), 3.971 (t, J = 5.4 Hz, 1H), 3.648 (s, 3H), 3.639 (s, 3H), 3.443 (dd, J = 4.2 Hz, J = 10.8 Hz, 1H), 3.274 (dd, J = 4.2 Hz, J = 10.8 Hz, 1H), 2.886 (d, J = 4.5 Hz, 2H), 2.796 (d, J = 4.2 Hz, 2H), 1.465 (s, 3H), 1.377 (s, 3H). ^{13}C NMR (DMSO-d_6, 75 MHz) δ/ppm = 171.020, 170.979, 169.866, 135.911, 134.762, 132.424, 121.631, 120.606, 118.463, 113.515, 110.914, 71.054, 56.511, 52.637, 51.747, 50.074, 41.223, 34.407, 24.583, 23.501, 23.280. $[\alpha]_D^{20} = -76$ (c = 0.23, acetone).

Dimethyl 1,2,3,5,11,11a-Hexahydro-3,3-dimethyl-1-oxo-6*H*-imidazo-[3′,4′:1,2]- pyridin[3,4-*b*]indol-2-glutarate (4j). Yield: 0.84 g (48%) as colorless powder; mp 234−236 °C. ESI/MS (*m*/*e*) 414 $[M + H]^+$. ^{1}H NMR ($CDCl_3$, 300 MHz) δ/ppm = 8.775 (s, 1H), 7.472 (t, J = 7.5 Hz, 1H), 7.293 (t, J = 7.5 Hz, 1H), 7.078 (d, J = 7.5 Hz, 1H), 7.046 (d, J = 7.5 Hz, 1H), 4.134 (t, J = 4.7 Hz, 1H), 3.904 (t, J = 5.6 Hz, 1H), 3.716 (s, 3H), 3.677 (s, 3H), 3.486 (dd, J = 4.2 Hz, J = 10.3 Hz, 1H), 3.116 (dd, J = 4.2 Hz, J = 10.3 Hz, 1H), 2.749 (d, J = 5.6 Hz, 2H), 2.681 (d, J = 4.7 Hz, 2H), 2.496 (d, J = 4.7 Hz, 2H), 1.473 (s, 3H), 1.367 (s, 3H). $_{13}$C NMR (DMSO-d_6, 75 MHz) δ/ppm = 171.026, 170.983, 169.870, 135.915, 134.770, 132.430, 121.637, 120.612, 118.469, 113.521, 110.922, 71.062, 56.517, 52.643, 51.751, 50.080, 41.231, 34.415, 26.887, 24.599, 23.507, 23.288. $[\alpha]_D^{20} = -58$ (c = 0.24, acetone).

Methyl (11a*S*)-1,2,3,5,11,11a-Hexahydro-3,3-dimethyl-1-oxo-6*H*-imidazo-[3′,4′:1,2]pyridin[3,4-*b*]indol-2-(2′*S*)-(hydroxymethyl)acetate (4k). Yield: 0.89 g (52%) as colorless powder; mp 196−197 °C. ESI/MS (*m*/*e*) 358 $[M + H]^+$. ^{1}H NMR ($CDCl_3$, 300 MHz) δ/ppm = 8.857 (s, 1H), 7.409 (t, J = 7.4 Hz, 1H), 7.293 (t, J = 7.4 Hz, 1H), 7.014 (d, J = 7.4 Hz, 1H), 6.971 (d, J = 7.4 Hz, 1H), 5.012 (t, J = 5.4 Hz, 1H), 4.176 (t, J = 5.4 Hz, 2H), 4.094 (t, J = 4.4 Hz, 1H), 3.814 (dd, J = 4.2 Hz, J = 10.2 Hz, 1H), 3.623 (s, 3H), 3.440 (dd, J = 4.2 Hz, J = 10.2 Hz, 1H), 2.879 (d, J = 4.4 Hz, 2H), 2.453 (s, 1H), 1.375 (s, 3H), 1.307 (s, 3H). ^{13}C NMR ($CDCl_3$, 75 MHz) δ/ppm = 170.987, 169.446, 135.911, 132.556, 126.663, 120.573, 118.438, 117.499, 110.897, 105.886, 78.137, 58.390, 56.816, 56.511, 52.044, 41.445, 24.492, 23.338, 19.275. $[\alpha]_D^{20} = -66$ (c = 0.22, acetone).

Methyl (11a*S*)-1,2,3,5,11,11a-Hexahydro-3,3-dimethyl-1-oxo-6*H*-imidazo-[3′,4′:1,2]pyridin[3,4-*b*]indol-2-(2′*S*,3′*R*)-(1-hydroxylethyl)acetate (4l). Yield: 0.72 g (42%) as colorless powder; mp 196−197 °C. ESI/MS (*m*/*e*) 372 $[M + H]^+$. ^{1}H NMR ($CDCl_3$, 300 MHz) δ/ppm = 8.669 (s, 1H), 7.403 (t, J = 7.5 Hz, 1H), 7.290 (t, J = 7.5 Hz, 1H), 7.010 (d, J = 7.5 Hz, 1H), 6.975 (d, J = 7.5 Hz, 1H), 5.010 (t, J = 5.5 Hz, 1H), 4.173 (m, J = 5.6 Hz, 1H), 4.097 (d, J = 4.6 Hz, 1H), 3.811 (dd, 1H, J = 4.3 Hz, J = 10.1 Hz, 1H), 3.620 (s, 3H), 3.435 (dd, 1H, J = 4.3 Hz, J = 10.1 Hz, 1H), 2.879 (d, 1H, J = 5.5 Hz, 2H), 2.453 (s, 1H), 1.375 (s, 3H), 1.307 (s, 3H), 1.286 (d, J = 4.6 Hz, 3H). ^{13}C NMR ($CDCl_3$, 75 MHz) δ/ppm = 171.544, 170.135, 136.037, 132.598, 126.685, 120.623, 118.608, 117.637, 111.229, 106.104, 78.715, 65.466, 58.412, 57.159, 56.573, 52.119, 41.607, 24.513, 23.357, 19.286. $[\alpha]_D^{20} = -85$ (c = 0.28, acetone).

Methyl (11a*S*)-1,2,3,5,11,11a-Hexahydro-3,3-dimethyl-1-oxo-6*H*-imidazo-[3′,4′:1,2]pyridin[3,4-*b*]indol-2-(2′*S*)-(aminocarbonylmethyl)acetate (4m). Yield: 0.69 g (40%) as colorless powder; mp 196−197 °C. ESI/MS (*m*/*e*) 385 $[M + H]^+$. ^{1}H NMR ($CDCl_3$, 300 MHz) δ/ppm = 8.770 (s, 1H), 7.413 (t, J = 7.4 Hz, 1H), 7.322 (t, J = 7.4 Hz, 1H), 7.012 (d, J = 7.4 Hz, 1H), 6.998 (d, J = 7.4 Hz, 1H), 6.217 (s, 2H), 4.559 (t, J = 4.7 Hz, 1H), 3.956 (t, J = 5.6 Hz, 1H), 3.667 (s, 3H), 3.450 (dd, J = 4.0 Hz, J = 10.1 Hz, 1H), 3.277 (dd, J = 4.0 Hz, J = 10.1 Hz, 1H), 2.883 (d, J = 5.6 Hz, 2H), 2.790 (d, J = 4.7 Hz, 2H), 1.460 (s, 3H), 1.375 (s, 3H). ^{13}C NMR (DMSO-d_6, 75 MHz) δ/ppm = 177.111, 172.968, 171.875, 135.937, 134.776, 132.431, 121.650, 120.614, 118.469, 113.522, 111.033, 71.107, 56.583, 51.145, 46.220, 45.588, 34.996, 24.617, 23.511, 23.289. $[\alpha]_D^{20} = -57$ (c = 0.24, acetone).

Methyl (11a*S*)-1,2,3,5,11,11a-Hexahydro-3,3-dimethyl-1-oxo-6*H*-imidazo-[3′,4′:1,2]pyridin[3,4-*b*]indol-2-(2′*S*)-(aminocarbonylethyl)acetate (4n). Yield: 0.78 g (45%) as colorless powder; mp 234−236 °C. ESI/MS (*m*/*e*) 399 $[M + H]^+$. ^{1}H NMR ($CDCl_3$, 300 MHz) δ/ppm = 8.771 (s, 1H), 7.468 (t, J = 7.5 Hz, 1H), 7.290 (t, J = 7.5 Hz, 1H), 7.072 (d, J = 7.5 Hz, 1H), 7.041 (d, J = 7.5 Hz, 1H), 6.231 (s, 2H), 4.132 (t, J = 4.8 Hz, 1H), 3.913 (t, J = 5.5 Hz, 1H), 3.681 (s, 3H), 3.482 (dd, J = 4.4 Hz, J = 10.1 Hz, 1H), 3.120 (dd, J = 4.4 Hz, J = 10.1 Hz, 1H), 2.745 (d, J = 5.5 Hz, 2H), 2.683 (m, J = 4.8 Hz, 2H), 2.492 (t, J = 4.8 Hz, 2H), 1.475 (s, 3H), 1.363 (s, 3H). ^{13}C NMR (DMSO-d_6, 75 MHz) δ/ppm = 176.021, 172.987, 170.872, 135.933, 134.776, 132.438, 121.641, 120.636, 118.503, 113.765, 111.205, 71.154, 56.549, 52.687, 50.682, 44.898, 31.433, 25.881, 24.908, 23.514, 23.296. $[\alpha]_D^{20} = -63$ (c = 0.25, acetone).

Methyl (11a*S*)-1,2,3,5,11,11a-Hexahydro-3,3-dimethyl-1-oxo-6*H*-imidazo-[3′,4′:1,2]pyridin[3,4-*b*]indol-2-(2′*S*)-(3-guanidinopropyl)acetate (4o). Yield: 0.79 g (45%) as colorless powder; mp 196−197 °C. ESI/MS (*m*/*e*) 427 $[M + H]^+$. ^{1}H NMR ($CDCl_3$, 300 MHz) δ/ppm = 8.787 (s, 2H), 8.722 (s, 1H), 8.224 (s, 1H), 7.360 (t, J = 7.5 Hz, 1H), 7.279 (t, J = 7.5 Hz, 1H), 7.003 (d, J = 7.5 Hz, 1H), 6.957 (d, J = 7.5 Hz, 1H), 6.504 (s, 1H), 4.661 (t, J = 5.6 Hz, 1H), 4.018 (t, J = 4.8 Hz, 1H), 3.815 (dd, J = 4.2 Hz, J = 10.3 Hz, 1H), 3.628 (s, 3H), 3.439 (dd, J = 4.2 Hz, J = 10.3 Hz, 1H), 2.863 (d, J = 4.8 Hz, 2H), 2.589 (t, J = 4.6 Hz, 2H), 1.900 (m, J = 4.6 Hz, 2H), 1.574 (m, J = 4.6 Hz, 2H), 1.376 (s, 3H), 1.313 (s, 3H). ^{13}C NMR ($CDCl_3$, 75 MHz) δ/ppm = 173.402, 173.337, 172.194, 135.748, 135.100, 132.499, 122.600, 120.679, 119.643, 113.555, 111.717, 71.333, 60.706, 51.903, 50.417, 47.007, 40.665, 27.334, 27.008, 25.884, 24.510, 23.362. $[\alpha]_D^{20} = -82$ (c = 0.22, acetone).

Methyl (11a*S*)-1,2,3,5,11,11a-hexahydro-3,3-dimethyl-1-oxo-6*H*-imidazo-[3′,4′:1,2]pyridin[3,4-*b*]indol-2-(2′*S*)-(imidazol-4-ylmethyl)acetate (4p). Yield: 0.61 g (35%) as colorless powder; mp 204−206 °C. ESI/MS (*m*/*e*) 408 $[M + H]^+$. ^{1}H NMR ($CDCl_3$, 300 MHz) δ/ppm = 10.072 (s, 1H), 8.885 (s, 1H), 7.411 (s, 1H), 7.265 (t, J = 7.3 Hz, 1H), 7.184 (d, J = 7.3 Hz, 1H), 7.025 (d, J = 7.3 Hz, 1H), 7.009 (d, J = 7.3 Hz, 1H), 6.820 (s, 1H), 4.700 (dd, J = 4.3 Hz, J = 9.5 Hz, 1H), 3.823 (t, J = 4.8 Hz, 1H), 3.690 (s, 3H), 3.482 (m, J = 4.3 Hz, 2H), 3.193 (d, J = 4.3 Hz, 2H), 2.905 (d, J = 4.8 Hz, 2H), 1.442 (s, 3H), 1.400 (s, 3H). ^{13}C NMR (DMSO-d_6, 75 MHz) δ/ppm = 171.119, 170.992, 136.440,136.228, 135.175, 134.864, 132.007, 123.393, 121.800, 120.759, 120.204, 112.920, 111.432, 70.978, 59.889, 51.648, 50.971, 45.202, 27.698, 29.430, 23.758, 23.665. $[\alpha]_D^{20} = -88$ (c = 0.26, acetone).

Methyl (11a*S*)-1,2,3,5,11,11a-hexahydro-3,3-dimethyl-1-oxo-6*H*-imidazo-[3′,4′:1,2]pyridin[3,4-*b*]indol-2-(2′*S*)-(2-methylthioethyl)acetate (4q). Yield: 1.11 g (64%) as colorless powder; mp 190−191 °C. ESI/MS (*m*/*e*) 402 $[M + H]^+$. ^{1}H NMR ($CDCl_3$, 300 MHz) δ/ppm = 7.997 (s, 1H), 7.473 (t, J = 7.2 Hz, 1H), 7.292 (t, J = 7.2 Hz, 1H), 7.088 (d, J = 7.2 Hz, 1H), 7.023 (d, J = 7.2 Hz, 1H), 4.137 (t, J = 4.2 Hz, 1H), 3.928 (t, J = 5.2 Hz, 1H), 3.721 (s, 3H), 3.480 (dd, J = 4.5 Hz, J = 10.8 Hz, 1H), 3.139 (dd, J = 4.5 Hz,, J = 10.8 Hz, 1H), 2.809 (d, J = 5.2 Hz, 2H), 2.577 (m, J = 4.2 Hz, 2H), 2.415 (m, J = 4.2 Hz, 2H), 2.151 (s, 3H), 1.479 (s, 3H), 1.363 (s, 3H). ^{13}C NMR (DMSO-d_6, 75 MHz) δ/ppm = 171.804, 170.913, 136.249, 131.148, 127.134, 121.637, 119.535, 118.085, 110.766, 108.005, 78.442, 57.294, 52.629, 52.514, 41.726, 31.481, 28.663, 24.806, 23.528, 22.951, 15.097. $[\alpha]_D^{20} = -102$ (c = 0.25, acetone).

In Vitro Vasodilation Assay. A constant temperature trough (CS501, Chongqing YinHe Experimental Apparatus Ltd. of China) was used to ensure the buffer warmed; a tension transducer (Hang JZ101, Beidian Xinghang Machine and Equipment Ltd.) and a two-channel physiological recorder (LMS-2B, Chengdu Apparatus Manufacturer) were used to evaluate the vasodilative effect. The male Wistar rats weighing 250−300 g (purchased from Animal Center of Capital Medical University) were used. Immediately after decapitation, rat aortic strips were taken and put in a perfusion bath

with 15 mL warmed (37 °C), oxygenated (95%O_2/5%CO_2) Kreb's solution (pH 7.4). The aortic strip was connected to a tension transducer, and the relaxation contraction curve of muscles was registered. Administration of 59 μM NE induced hypertonic contraction of the vessel strip. As the contraction reaches its maximum, NE was washed out, and the vessel strip was stabilized for 30 min. After renewal of the solution, 59 μM NE was added. When the hypertonic contraction value of the aortic strip reached the peak (the highness was taken as 100% contraction), 15 μL of ethanol (negative control), or 15 μL solution of tadalafil in ethanol (positive control) or 15 μL solution of Ach in ethanol (positive control) or 15 μL solution of **4a**−**q** in ethanol was administrated to observe the vasodilation and the percent of vasodilation was taken as the vasorelaxation activity.

Acknowledgment. This work was supported by Beijing Area Major Laboratory of Peptide and Small Molecular Drugs, the 973 Project of China (2006CB708501), and the National Natural Scientific Foundation of China (30672513).

Supporting Information Available: Summary of crystal data and details of intensity collection of **4f**,**h** and elemental analysis data of **3a**−**q** and **4a**−**q**. This material is available free of charge via the Internet at http://pubs.acs.org.

References

(1) Johnsson, E.; Maddahi, A.; Wackenfors, A.; Edvinsson, L. Enhanced expression of contractile endothelin ETB receptors in rat coronary artery after organ culture. *Eur. J. Pharmacol.* **2008**, *582*, 94–101.
(2) Stephen, Y.; Chan, A. C.; Loscalzo, J. Pathogenic mechanisms of pulmonary arterial hypertension. *J. Mol. Cell. Cardiol.* **2008**, *44*, 14–30.
(3) Roux, S.; Loffler, B. M.; Gray, G. A.; Sprecher, U.; Clozel, M.; Clozel, J. P. The role of endothelin in experimental cerebral vasospasm. *Neurosurgery* **1995**, *37*, 78–85.
(4) Henriksson, M.; Stenman, E.; Edvinsson, L. Intracellular pathways involved in upregulation of vascular endothelin type B receptors in cerebral arteries of the rat. *Stroke* **2003**, *34*, 1479–1483.
(5) Wackenfors, A.; Emilson, M.; Ingemansson, R.; Hortobagyi, T.; Szok, D.; Tajti, J.; Vecsei, L.; Edvinsson, L.; Malmsjo, M. Ischemic heart disease induces upregulation of endothelin receptor mRNA in human coronary arteries. *Eur. J. Pharmacol.* **2004**, *484*, 103–109.
(6) Dagassan, P. H.; Breu, V.; Clozel, M.; Kunzli, A.; Vogt, P.; Turina, M.; Kiowski, W.; Clozel, J. P. Up-regulation of endothelin-B receptors in atherosclerotic human coronary arteries. *J. Cardiovasc. Pharmacol.* **1996**, *27*, 147–153.
(7) Beavo, J. A. Cyclic nucleotide phosphodiesterases: functional implications of multiple isoforms. *Physiol. Rev.* **1995**, *75*, 725–748.
(8) Conti, M.; Jin, S. L. The molecular biology of cyclic nucleotide phosphodiesterases. *Prog. Nucleic Acid Res. Mol. Biol.* **1999**, *63*, 1–38.
(9) Houslay, M. D. Adaptation in cyclicAMP signalling processes: a central role for cyclic AMP phosphodiesterases. *Semin. Cell Dev. Biol.* **1998**, *9*, 161–167.
(10) Francis, S. H.; Turko, I. V.; Corbin, J. D. Cyclic nucleotide phosphodiesterases: relating structure and function. *Prog. Nucleic Acid Res. Mol. Biol.* **2001**, *65*, 1–52.
(11) Corbin, J. D.; Francis, S. H. Pharmacology of phospho diesterase-5 inhibitors. *Int. J. Clin. Pract.* **2002**, *56*, 453–459.
(12) Rotella, D. P. Phosphodiesterase 5 inhibitors: current status and potential applications. *Nat. Rev. Drug Discovery* **2002**, *1*, 674–682.
(13) Conti, M. Phosphodiesterases and cyclic nucleotide signaling in endocrine cells. *Mol. Endocrinol.* **2000**, *14*, 1317–1327.
(14) Mehats, C.; Andersen, C. B.; Filopanti, M.; Jin, S. L.; Conti, M. Cyclic nucleotide phosphodiesterases and their role in endo crine cell signaling. *Trends Endocrinol. Metab.* **2002**, *13*, 29–35.
(15) Corbin, J. D.; Francis, S. H. Cyclic GMP phosphodiesterase-5: target of sildenafil. *J. Biol. Chem.* **1999**, *274*, 13729–13732.
(16) Ballard, S. A.; Gingell, C. J.; Tang, K.; Turner, L. A.; Price, M. E.; Naylor, A. M. Effects of sildenafil on the relaxation of human corpus cavernosum tissue in vitro and on the activities of cyclic nucleotide phosphodiesterase isozymes. *J. Urol.* **1998**, *159*, 2164–2171.
(17) Haning, H.; Niewohner, U.; Schenke, T.; Es-Sayed, M.; Schmidt, G.; Lampe, T.; Bischoff, E. Imidazo[5,1-*f*]triazin-4(3*H*)-ones, a new class of potent PDE 5 inhibitors. *Bioorg. Med. Chem. Lett.* **2002**, *12*, 865–868.
(18) Porst, H. IC351 (tadalafil, Cialis): update on clinical experience. *Int. J. Impot. Res.* **2002**, *14*, S57–S64.
(19) Card, G. L.; England, B. P.; Suzuki, Y.; Fong, D.; Powell, B.; Lee, B.; Luu, C.; Tabrizizad, M.; Gillette, S.; Ibrahim, P. N.; Artis, D. R.; Bollag, G.; Milburn, M. V.; Kim, S. H.; Schlessinger, J.; Zhang, K. Y. J. Structural Basis for the Activity of Drugs that Inhibit Phosphodiesterases. *Structure* **2004**, *12*, 2233–2247.
(20) Gitto, R.; Ficarra, R.; Stancanelli, R.; Guardo, M.; De Luca, L.; Barreca, M. L.; Pagano, B.; Rotondo, A.; Bruno, G.; Russo, E.; De Sarroc, G.; Chimirri, G. A. Synthesis, resolution, stereochemistry, and molecular modeling of (*R*)- and (*S*)-2-acetyl-1-(40-chlorophenyl)-6,7-dimethoxy-1,2,3,4-tetrahydroisoquinoline AMPAR antagonists. *Bioorg. Med. Chem.* **2007**, *15*, 5417–5423.
(21) Shaikh, A. R.; Ismael, M.; Carpio, C. A. D.; Tsuboi, H.; Koyama, M.; Endou, A.; Kubo, M.; Broclawikc, E.; Miyamoto, A. Three-dimensional quantitative structure- activity relationship (3D-QSAR) and docking studies on (benzothiazole-2-yl)acetonitrile derivatives as c-Jun N-terminal kinase-3 (JNK3) inhibitors. *Bioorg. Med. Chem. Lett.* **2006**, *16*, 5917–5925.
(22) Doddareddy, M. R.; Cho, Y. S.; Koh, H. Y.; Pae, A. N. CoMFA and CoMSIA 3D QSAR analysis on N1-arylsulfonylindole compounds as 5-HT6 antagonists. *Bioorg. Med. Chem.* **2004**, *12*, 3977–3985.
(23) Sharma, S. K.; Kumar, G.; Kapoor, M.; Surolia, A. Combined effect of epigallo-catechin gallate and triclosan on enoyl-ACP reductase of Mycobacterium tuberculosis. *Biochem. Biophy. Res. Commun.* **2008**, *368*, 12–17.
(24) Liu, J.; Cui, G.; Zhao, M.; Cui, C.; Ju, J.; Peng, S. Dual-acting agents that possess reversing resistance and anticancer activities: Design, synthesis, MES-SA/Dx5 cell assay, and SAR of benzyl 1,2,3,5,11,11a-hexahydro-3,3-dimethyl-1-oxo-6*H*-imidazo[3′,4′:1,2]pyridin[3,4-*b*]indol-2-substituted acetates. *Bioorg. Med. Chem.* **2007**, *15*, 7773–7788.

JM800249J